Mineralogical Magazine, October 2018, Vol. 82(5), pp. 1057–1077

Ammoniovoltaite, $(NH_4)_2Fe^{2+}_5Fe^{3+}_3Al(SO_4)_{12}(H_2O)_{18}$, a new mineral from the Severo-Kambalny geothermal field, Kamchatka, Russia

Elena S. Zhitova[1,2,*], Oleg I. Siidra[1,3], Dmitry I. Belakovsky[4], Vladimir V. Shilovskikh[5], Anton A. Nuzhdaev[2] and Rezeda M. Ismagilova[1]

[1] Department of Crystallography, St. Petersburg State University, Universitetskaya nab. 7/9, St. Petersburg 199034, Russia
[2] Geothermal laboratory, Institute of Volcanology and Seismology, Russian Academy of Sciences, Bulvar Piypa 9, Petropavlovsk-Kamchatsky 683006, Russia
[3] Nanomaterials Research Center, Kola Science Center, Russian Academy of Sciences, Apatity, Murmansk region, 184200, Russia
[4] Fersman Mineralogical Museum, Leninsky prospect 18-2, Moscow 117071, Russia
[5] Resource Center, St. Petersburg State University, Universitetskaya nab. 7/9, St. Petersburg 199034, Russia

[*Received 23 July 2017; Accepted 16 October 2017; Associate Editor: Anthony Kampf*]

Abstract

Ammoniovoltaite, $(NH_4)_2Fe^{2+}_5Fe^{3+}_3Al(SO_4)_{12}(H_2O)_{18}$, is a new voltaite-group mineral. The mineral was discovered at the Severo-Kambalny (North-Kambalny) geothermal field, Kambalny volcanic ridge, Southern Kamchatka, Russia. Ammoniovoltaite forms at ~100°C around geothermal gas/steam vents in association with alunogen, tschermigite and pyrite. Crystals of ammoniovoltaite have euhedral habit, are up to 50 μm in size and grow on alunogen plates. Ammoniovoltaite is black with vitreous lustre, opaque, brittle and water-soluble. Neither cleavage nor parting is found, the fracture is conchoidal. The mineral is isotropic, with the refractive index $n = 1.602(2)$ (589 nm). Infrared spectra contain an absorption band at 1433 cm^{-1} distinctive for the ammonium ion. The chemical composition is (iron content is given in accordance with Mössbauer data, H_2O calculated from a crystal-structure refinement, wt.%): FeO 13.26, Fe_2O_3 11.58, MgO 2.33, ZnO 0.04, Al_2O_3 2.74, SO_3 47.46, K_2O 0.19, CaO 0.11, $(NH_4)_2O$ 2.96, H_2O 16.03, total 96.70. The empirical formula based on S = 12 atoms per formula unit is $[(NH_4)_{1.88}K_{0.08}Ca_{0.04}]_{\Sigma 2.00}(Fe^{2+}_{3.74}Mg_{1.17}Fe^{3+}_{0.05}Zn_{0.01})_{\Sigma 4.97}(Fe^{3+}_{2.89}Al_{0.09})_{\Sigma 2.98}Al_{1.00}(SO_4)_{12.00}(H_2O)_{18.00}$. The crystal structure has been refined to $R_1 = 0.031$ and 0.030 on the basis of 1217 and 1462 unique reflections with $I > 2\sigma(I)$ collected at 100 K and room temperature, respectively. Ammoniovoltaite is the ammonium analogue of voltaite. The mineral is cubic, $Fd\bar{3}c$, $a = 27.250(1)$ Å and $V = 20234(3)$ Å^3 (at 100 K); and $a = 27.322(1)$ Å and $V = 20396(3)$ Å^3 (at RT), with $Z = 16$. The strongest lines of the powder X-ray diffraction pattern [*d*, Å (*I*, %) (*hkl*)] are: 9.67 (74) (022), 7.90 (56) (222), 5.58 (84) (422), 3.560 (100) (731), 3.418 (100) (008) and 2.8660 (37) (931). A brief review of ammonium minerals from various volcanically active geological environments is given.

Keywords: ammoniovoltaite, sulfate, ammonium, new mineral, voltaite group, geothermal field, Kambalny volcano.

Introduction

The southern part of Kamchatka Peninsula is famous for a large number of geothermal fields (Fig. 1) (Rychagov *et al.*, 2014). The latter have been studied extensively due to the high potential for geothermal energy. The area around Kambalny volcano is well-known for geothermal activity with the emissions of CO_2, H_2S and CH_4 gases. The surface of the Severo-Kambalny geothermal field (as well as other geothermal fields in Southern Kamchatka) is usually covered by efflorescences

*E-mail: zhitova_es@mail.ru
https://doi.org/10.1180/minmag.2017.081.083

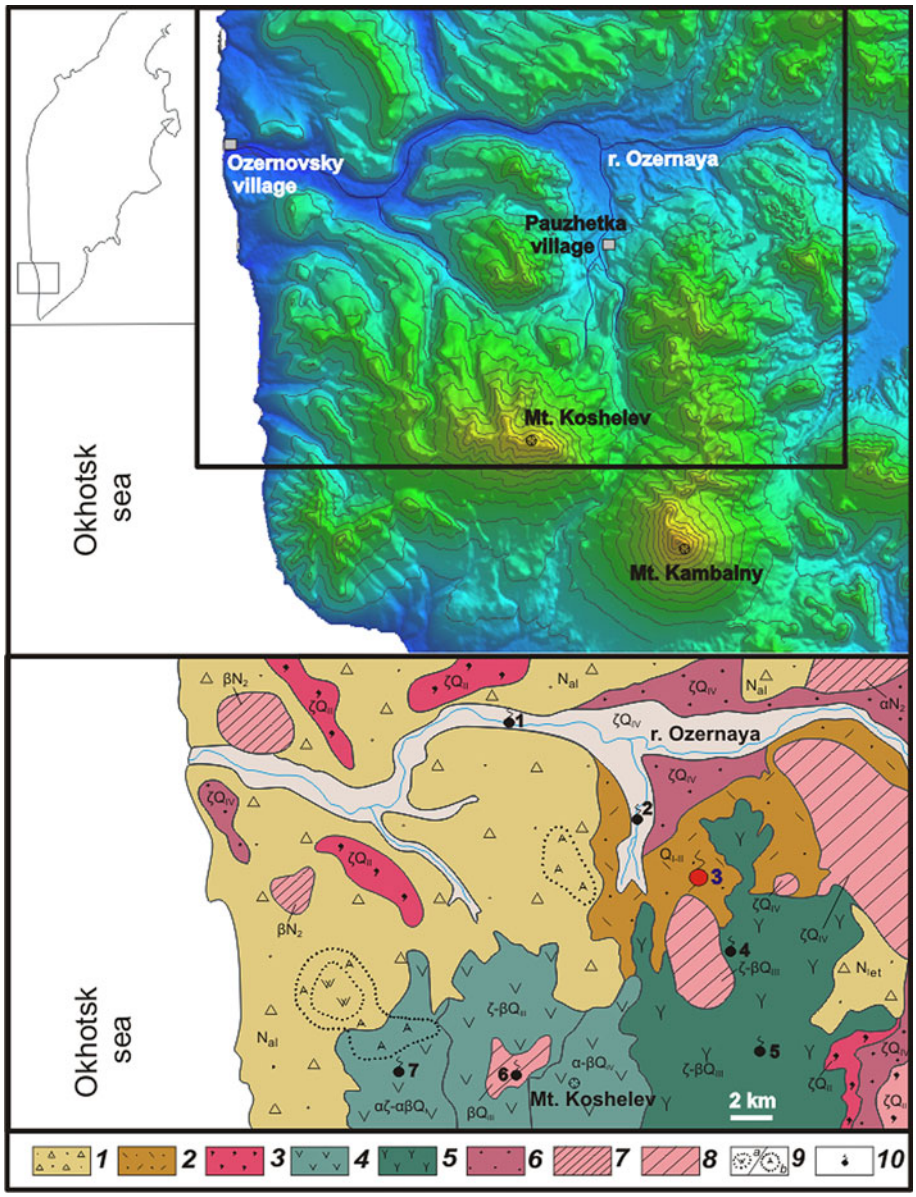

FIG. 1. Geographical (upper) and geological (lower) maps of the south-western part of Kamchaka Peninsula (Rychagov *et al*., 2014). Key: (1) 1ava-pyroclastic sediments of Neogene age; (2) volcanogenic-sedimentary rocks (tuffites) of Pauzhetka suite; (3) ignimbrites; (4) lava complexes of Koshelev volcanic massif; (5) volcanic rocks (lavas, pyroclastic flows and extrusions) of Kambalny ridge; (6) pumice dacite; (7) subvolcanic and extrusive bodies of basalt and andesite; (8) extrusive subvolcanic bodies of contrasting composition; (9) hydrothermally altered rocks: *A* – secondary quarzites, *W* – argillites; (10) geothermal fields: 1 – Perviye goryachuye istochniki, 2 – Pauzhetsky, 3 – Severo-Kambalny (marked by red spot), 4 – Central`no-Kambalny, 5 – Yuzhno-Kambalny, 6 – Verhne-Koshelevsky, 7 – Nizhne-Koshelevsky.

that originate under conditions of: (1) elevated temperature up to ~100°C; and/or (2) acid leaching of primary rocks with the release of elements for the subsequent formation of various exhalative minerals. Mineral assemblages of the Severo-Kambalny geothermal field are represented mostly by

water-soluble minerals, usually hydrated sulfates that only appear and remain stable in periods of dry weather. In 2014, uncommon for the region, relatively dry weather conditions occurred for several summer weeks and allowed discoveries of ammoniovoltaite.

Ammoniovoltaite and associated minerals described in this paper were found prior to the recent eruption of Kambalny volcano in March 2017. The Severo-Kambalny geothermal field is located ~15 km away from the active crater. Neither changes in dimensions nor in geochemical parameters (temperature, pH and Eh) were observed for the Severo-Kambalny field during the summer expeditions in 2014 and 2016 by the Geothermal Laboratory of Institute of Volcanology and Seismology, Russian Academy of Sciences.

Here we describe the new species ammoniovoltaite, ideally $(NH_4)_2Fe^{2+}_5Fe^{3+}_3Al(SO_4)_{12}(H_2O)_{18}$. The name highlights the composition of the mineral, i.e. ammonium analogue of voltaite. The mineral and its name have been approved by the International Mineralogical Association Commission on New Minerals, Nomenclature and Classification (IMA2017-022, Zhitova *et al*. 2017). The type specimen is deposited in the collections of the Fersman Mineralogical Museum of the Russian Academy of Sciences, Moscow, Russia, with the registration number 5030/1 (part of the holotype).

Occurrence

Ammoniovoltaite was found in the central part of the Severo-Kambalny geothermal field (51.42854°N, 156.87341°E), Kambalny volcanic ridge, Kamchatka Peninsula, Russia (Fig. 1). Geothermal fields related to Kambalny volcano are divided into three groups: Severo (=North)-, Yuzhno (=South)-, Central`no (=Central)-Kambalny without a unique name for each thermal anomaly. The Severo-Kambalny group consists of several rather weak and small thermal anomalies and a much larger active field, therefore the name Severo-Kambalny usually refers to the field. The Severo-Kambalny geothermal field (Fig. 2) is located at 900–950 m above sea level and has approximate dimensions of 200 m × 250 m.

Primary lava flows of andesite–basalt, andesite and dacite were converted to variegated clays (Rychagov *et al*., 2017) as a result of hydrothermal activity at the Severo-Kambalny geothermal field. Remnants of lava flows are very scarce (Fig. 2). The field is characterized by a number of gas/steam vents (up to 50 cm in diameter) and mudpots (up to 60 cm in diameter). The maximum temperatures of gas/steam vents and mudpots are 99°C and 103°C, respectively. The circulating hydrothermal solution is mainly acidic with pH ranging from 1.9 to 6.7.

The significant ammonium concentration at the geothermal fields in this area was first noted by Nekhoroschev (1959) and confirmed later by analyses that reported $(NH_4)^+$ in mudpots in the range 10.5–750 mg/l (Ogorodova *et al*., 1971). A high ammonium concentration in hydrothermal solution was also reported for geothermal fields associated with the neighbouring Koshelev volcano (Fig. 1) (Kalacheva *et al*., 2016).

Ammoniovoltaite covers walls in cracks around gas/steam vents in strongly hydrothermally altered remnants of andesite–basalt lava flows (Fig. 2). The temperature of gases at the sampling location was ~100°C. In general, Kambalny geothermal fields are characterized by a high content of pyrite (Rychagov *et al*., 2010) and the oxidation of primary sulfides causes the formation of secondary sulfates. The mineral is found in close association with alunogen, tschermigite and pyrite (Fig. 3).

General appearance and physical properties

Ammoniovoltaite occurs in aggregates or microscopic euhedral, usually distorted, crystals growing on alunogen plates (Figs 3, 4). The mineral exhibits the following forms: octahedral, cubo-octahedral and cubic (Fig. 4). Ammoniovoltaite is black with greenish grey colour in thin fragments, opaque to translucent and has a vitreous lustre (Fig. 3). The mineral is brittle. The Mohs hardness is ~3–3.5, estimated by: (1) analogy with other group members; and (2) crushing of the mineral grains between slides. Neither cleavage nor parting is observed and the fracture is conchoidal. The mineral is water-soluble and decomposes with formation of acid solution and solid residual.

Macroscopically the mineral is black, even in the smallest visible grains. In plain-polarized light, it is pale greenish-grey and nonpleochroic. Grains and their fragments have an equant shape and no cleavage was observed. The mineral is isotropic. The refractive index is $n = 1.602(2)$ (589 nm).

Infrared spectroscopy

Infrared (IR) spectra were obtained using the KBr pellet method (200 mg of KBr and 2 mg of

FIG. 2. General view (*a*) and remnants of lava flows covered by white alunogen (*b*, ~1 m by 2 m field of view) in the Severo-Kambalny geothermal field (Southern Kamchatka, Russia).

ammoniovoltaite) and a Bruker Vertex 70 FTIR spectrometer at room temperature.

The IR spectra are shown in Fig. 5. The main absorption bands and their tentative assignments are represented in Table 1 and are in good agreement with the data for ammoniomagnesiovoltaite $(NH_4)_2Mg_5Fe^{3+}_3Al(SO_4)_{12}(H_2O)_{18}$ (Szakáll *et al*., 2012, Chukanov, 2014) and synthetic $(NH_4)_2Fe^{2+}_5Fe^{3+}_3Al(SO_4)_{12}(H_2O)_{18}$ (denoted below as NH_4-Fe synthetic voltaite as reported in Majzlan *et al*., 2013). The spectra contain a broad and intensive band ~3400 cm^{-1} with a shoulder at 3300–2400 cm^{-1} previously attributed to stretching vibrations of OH (Szakáll *et al*., 2012, Chukanov *et al*., 2016) and NH_4 (Majzlan *et al*., 2013). The split bands at 1691 and 1641 cm^{-1} were assigned to H–O–H bending vibrations in water molecules. The band at 1433 cm^{-1} is a distinctive feature of ammonium in voltaites (Szakáll *et al*., 2012; Majzlan *et al*., 2013). Three split bands observed in the region 1200–1000 cm^{-1} (1124, 1053 and 1003 cm^{-1}) are due to asymmetric and symmetric stretching vibrations of sulfate (Szakáll *et al*., 2012). The bands at 893 and 727 cm^{-1} are attributed to Fe···O–H bending vibrations combined with overtones of Fe···O stretching vibrations. The bands in the region 660–590 cm^{-1} are assigned to SO_4 bending vibrations. The band at

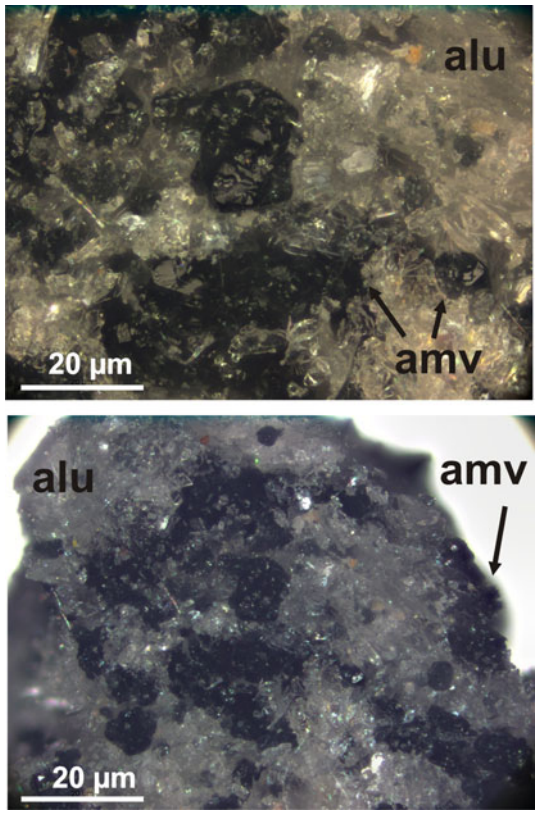

FIG. 3. Images of black ammoniovoltaite (amv) in association with white alunogen (alu) under an optical microscope.

438 cm^{-1} is due to $Fe^{3+}\cdots O$ bending vibrations and/or $\nu_2(E)$ bending vibrations of SO_4^{2-} (Chukanov *et al.*, 2016).

Mössbauer spectroscopy

Mössbauer spectra were collected at room temperature using a $^{57}Co(Rh)$ source. The spectrometer was calibrated using the spectra of α-Fe at room temperature. Powdered absorbers were pressed in plastic disks and fixed on an aluminium holder. The density of the natural iron in the absorber was <5 mg/cm^2. The spectra were analysed using a Voigt-based quadrupole-splitting distribution (QSD) analysis. The Lorentzian linewidth (Γ) of the symmetrical elemental doublet of the QSD was allowed to vary during the spectra fitting to account for absorber-thickness effects (*MossFit* software).

The Mössbauer spectra for ammoniovoltaite are shown in Fig. 6 and selected hyperfine parameters are given in Table 2. The spectra of ammoniovoltaite show absorption peaks due to both Fe^{2+} (the dominant species) and Fe^{3+}. It was fit to a QSD model having two generalized sites, one for Fe^{2+} (with one Gaussian component) and one for Fe^{3+} (with one Gaussian component) (Table 2). The comparative data for ammoniovoltaite and its synthetic analogue, NH_4-Fe voltaite, (Majzlan *et al.*, 2013) are given in Table 2 from which it can be inferred that Fe^{2+}:Fe^{tot} is 0.56 and 0.63 for ammoniovoltaite and its synthetic analogue, respectively. The observed difference originates from occupancy of the octahedral M^{2+} site that is populated exclusively by Fe in the synthetic compound (Majzlan *et al.*, 2013), whereas in ammoniovoltaite Mg occupies ~23% of M^{2+} (see below) affecting Fe^{2+}:Fe^{tot}.

Chemical composition

Crystals of ammoniovoltaite were mounted in an epoxy block and polished. The sample was coated with a 10 nm carbon layer for further electron microscopy work. Preliminary quantitative chemical analyses were performed by a scanning electron microscope Hitachi S3400N equipped with an Oxford X-Max 20 energy-dispersive spectrometer. Working conditions were 20 kV accelerating voltage and 1.5 nA beam current. Spectra were obtained at spot mode for 30 s each and revealed that the mineral contains abundant Fe, S, Al, Mg and N and minor Zn, K and Ca. The study of element distributions revealed zoning of ammoniovoltaite crystals mainly in the Fe/Mg ratio (21.08–27.18 wt.% FeO and 0.69–3.72 wt.% MgO) and minor variations in the content of K and Ca (0–0.27 wt.% K_2O and 0–0.24 wt.% CaO) (Fig. 7).

Further quantitative element analyses were performed using a scanning electron microscope Hitachi S3400N equipped with an INCA Wave 500 wavelength-dispersive spectrometer (WDS). Operating conditions were as follows: acceleration voltage 20 kV, probe current 10 nA and peak and background acquisition were 30 s and 15 s, respectively. Ammoniovoltaite is unstable under a spot electron beam. Therefore, a defocused beam (5 μm × 5 μm spot size) was used for the analyses. Raw intensity data were corrected using a matrix correction by the 'XPP' method (modified φ(ρZ), Pouchou and Pichoir, 1991). For WDS standardization the following reference compounds were used: FeS_2 for iron, MgO for magnesium, Zn for zinc, Al_2O_3 for aluminium, $CaSO_4$ for calcium,

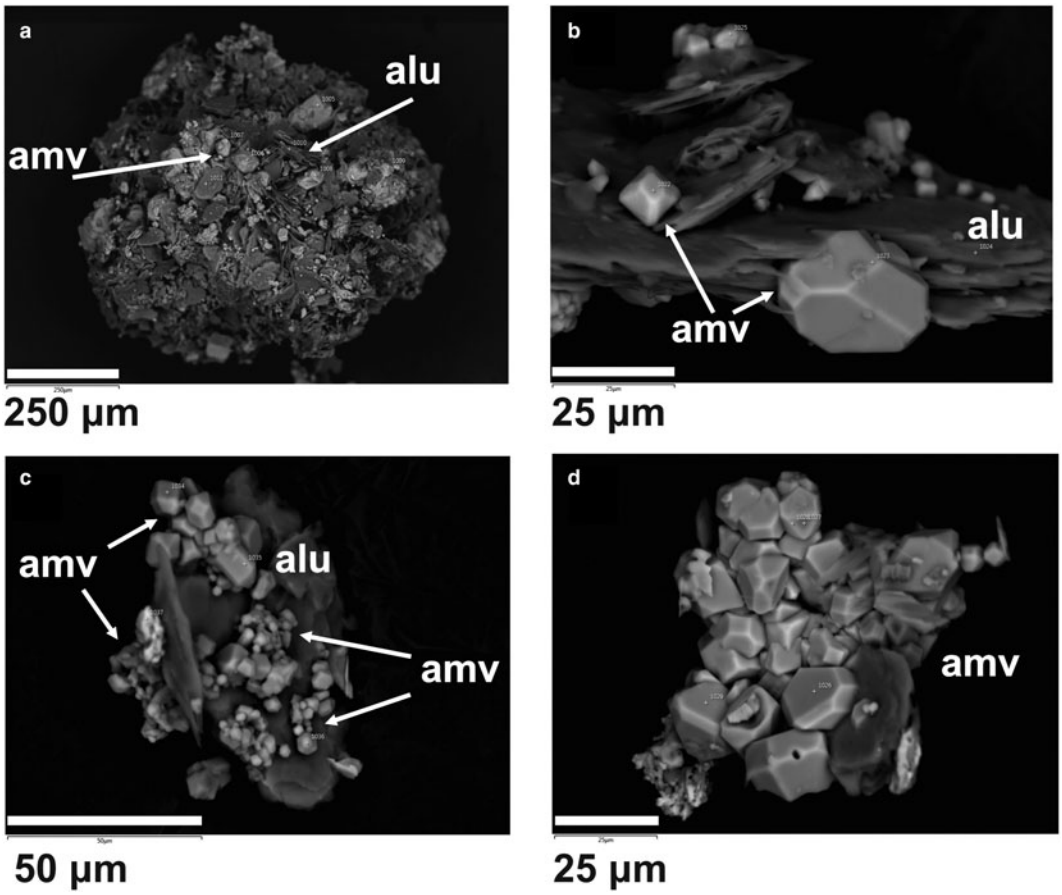

FIG. 4. Back-scatter electron images of ammoniovoltaite (amv) in association with lammellar aggregates of alunogen (alu).

KCl for potassium and $CaSO_4$ for sulfur. The chemical composition averaged for six analyses is given in Table 3. It was impossible to separate pure material in the amount sufficient for direct quantitative determination of N and H by gas chromatography. Therefore the amount of N was measured in energy-dispersive spectroscopy (EDS) mode by scanning electron microscopy using BN as the standard. The measurement gave a somewhat overestimated value for N (Table 3). Therefore it was reduced in the chemical formula based on charge-balancing or $(NH_4) + Ca + K = 2$ atoms per formula unit (apfu) (supported by single-crystal structure refinement). The amount of H_2O was calculated based on the crystal-structure data. The empirical chemical formula calculated on the basis of S = 12 apfu is $[(NH_4)_{1.88}K_{0.08}Ca_{0.04}]_{\Sigma 2.00}(Fe^{2+}_{3.74}Mg_{1.17}Fe^{3+}_{0.05}Zn_{0.01})_{\Sigma 4.97}(Fe^{3+}_{2.89}Al_{0.09})_{\Sigma 2.98}Al_{1.00}(SO_4)_{12.00}(H_2O)_{18.00}$. The simplified formula is $(NH_4)_2Fe^{2+}_5Fe^{3+}_3Al(SO_4)_{12}(H_2O)_{18}$. The Gladstone-Dale compatibility index $1-(K_P/K_C) = -0.015$ (superior, for $(NH_4)_2O$ – 2.96 wt.% [measured]) (Mandarino, 2007).

Powder X-ray diffraction

Preliminary powder X-ray diffraction (XRD) patterns were obtained by means of a Bruker D2 Phaser diffractometer in Bragg-Brentano geometry operated at 30 kV/10 mA, LYNXEYE detector (Cu$K\alpha$, step scan = 0.02°, counting time = 1 s and 2θ range of 5–55°) and revealed the presence of a voltaite-group mineral, alunogen and tschermigite.

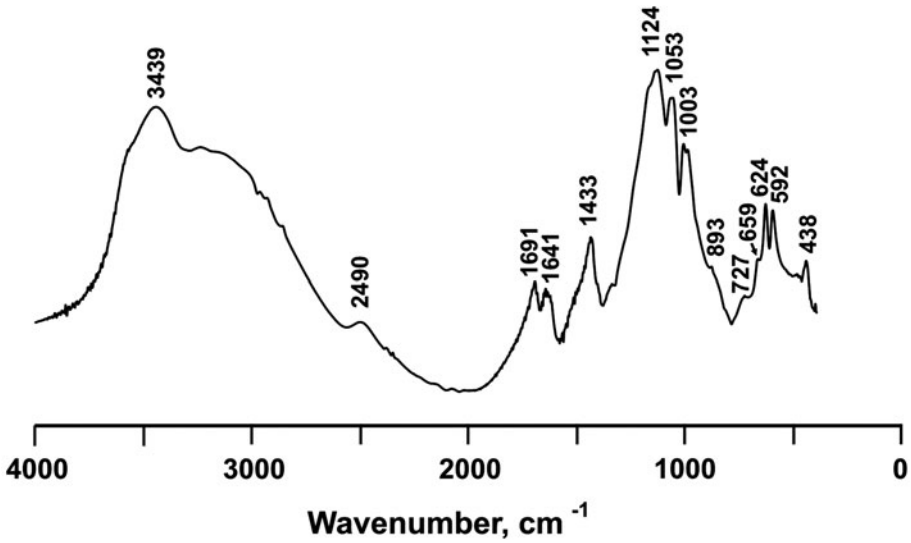

FIG. 5. IR spectrum of ammoniovoltaite.

Due to the coexistence with tschermigite, ammonium substitution in the voltaite-group mineral was considered to be very probable. The black colour of the mineral indicated that it is not ammoniomagnesiovoltaite which is yellow.

Several crystals of ammoniovoltaite were crushed and mounted in Paraton oil in a loop. The sample was studied by Gandolfi-like motion using a Rigaku RAXIS RAPID II diffractometer (Debye-Scherrer geometry, $d = 127.4$ mm) equipped with a rotating anode X-ray source (Co$K\alpha$) and a curved image plate detector. The data were integrated using the software package *Osc2Tab/SQRay* (Britvin *et al*., 2017). *Topas 4.2* (Bruker-AXS 2009) was used for the refinement of the unit-cell parameters of ammoniovoltaite by the Rietveld method and for indexing of powder XRD data. The structural model in the $Fd\bar{3}c$ space group of the synthetic analogue of ammoniovoltaite (Majzlan *et al*., 2013) was used initially. Unit-cell parameters refined from the powder XRD data are $a = 27.352(1)$ Å and $V = 20462(3)$ Å^3. Indexed powder XRD data are provided in Table 4.

Single-crystal XRD

Single-crystal XRD data for structure determination were collected at 100 K and room temperature (RT) for two different crystals with Mo$K\alpha$ radiation by means of a Bruker APEX II DUO diffractometer operated at 50 kV/40 mA and equipped with a CCD area detector. The data were collected and processed using the Bruker software *APEX2* (Bruker-AXS, 2014); details on data collection are in Table 5. A semi-empirical absorption-correction based upon the intensities of equivalent reflections was applied (*SADABS*, Sheldrick, 2015). The diffraction data were indexed in space group $Fd\bar{3}c$ with $a = 27.250$ (1) Å at 100 K and $a = 27.322(1)$ Å at RT (Table 5). The atomic coordinates, isotropic displacement parameters and site occupancies are given in Table 6, anisotropic displacement parameters are provided in Table 7. Selected bond distances are listed in Table 8. The crystallographic information files have been deposited with the Principal Editor of *Mineralogical Magazine* and are available as Supplementary material (see below).

The structure refinements were performed using S*HELXL* software (Sheldrick, 2015). The initial atomic coordinates for the structure refinements were taken from the structure reports of voltaite published by Mereiter (1972) and Majzlan *et al*. (2013) except for the $O6_w$ and $O7_w$ sites and hydrogen atoms of the $O5_w$ oxygen atom belonging to water molecules. All non-hydrogen atoms were refined anisotropically. Although several peaks are observed around the *A* site ($A = N_{0.96}K_{0.02}Ca_{0.02}$), hydrogen atoms of the ammonium group were removed from the refinement as they are strongly

TABLE 1. Wavenumbers (cm^{-1}) of absorption bands in the IR spectra of ammoniovoltaite in comparison to its synthetic analogue and ammoniomagnesiovoltaite.

Ammoniovoltaite $(NH_4)_2Fe^{2+}_5Fe^{3+}_3Al(SO_4)_{12}(H_2O)_{18}$ This work	Ammoniomagnesiovoltaite $(NH_4)_2Mg_5Fe^{3+}_3Al(SO_4)_{12}(H_2O)_{18}$ Szakáll *et al.* (2012)	Ammoniomagnesiovoltaite $(NH_4)_2Mg_5Fe^{3+}_3Al(SO_4)_{12}(H_2O)_{18}$ Chukanov (2014)	Synthetic $(NH_4)_2Fe^{2+}_5Fe^{3+}_3Al(SO_4)_{12}(H_2O)_{18}$ Majzlan *et al.* (2013)	Tentative assignment in accordance with Chukanov *et al.* (2016)
3439 3300–2600	3423 ~3263	3550, 3380 3215, 3120	3560–3000 ~3248, 3091	Stretching of OH and NH_4
2490	n.a.	2500	2501	O–H stretching in acid sulfate groups*
1691 1641	n.a. 1641	1693 1635	1689 1639	H_2O bending
1433	1431	1430	1431	NH_4
1124 1053	1122 1065	1215, 1152 1068	1153, 1130 1055	SO_4 asymmetric stretching
1003	1014	1002	1007	SO_4 symmetric stretching
893 727	n.a.	885 710	879 731	Fe···O–H bending combined with overtones of Fe···O stretching
659 624 592	n.a. 594	656 629 595	– 627 592	SO_4 bending
438	474	505, 465, 445	442	Fe^{3+}···O bending and/or $\nu_2(E)$ bending of SO_4^{2-}

'n.a.' – Observed but wavenumber is not provided.
*As a result of reversible proton transfer $SO_4^{2-} + H_2O \leftrightarrow HSO_4^- + OH^-$ (the low intensity of this band indicates that the dynamic chemical equilibrium is strongly shifted to the left).

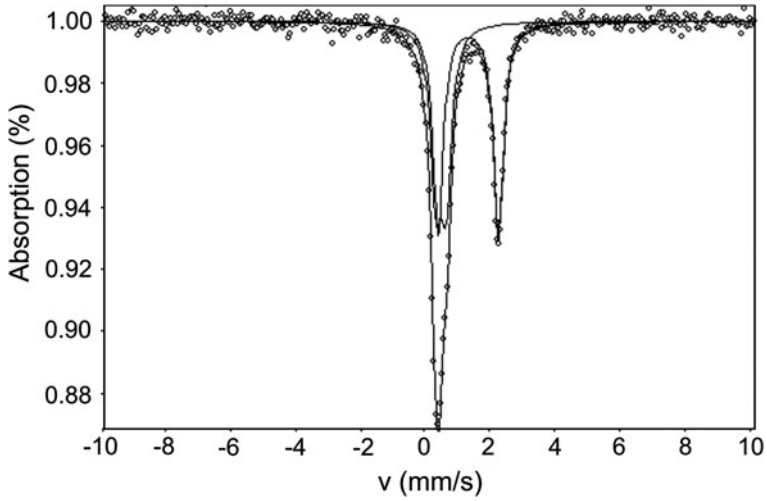

FIG. 6. Mössbauer spectra of ammoniovoltaite.

disordered. Site occupancies of the mixed- and partially occupied sites *A*, *M*1 and *M*2 were refined (Table 6). Hydrogen atoms for the $O5_w$ water molecule were located from the difference-Fourier map, the O–H bonds were softly restrained at the distance 0.96(4) Å.

The bond-valence sums in valence units (vu) are 3.00 for *M*1, 2.26 for *M*2, 3.21 for Al and 5.98 for S sites calculated using bond-valence parameters from Gangé and Hawthorne (2015). The bond-valence sums were calculated on the basis of the following assumed site occupancies: $M1 = Fe^{3+}$, $M2 = Fe^{2+}_{0.62}Mg_{0.20}Fe^{3+}_{0.17}Zn_{0.01}$, S = S and Al = Al. A bond-valence sum for the *A* site was not calculated as hydrogen atoms of ammonium groups were not localized.

Description of the crystal structure

The crystal structure of ammoniovoltaite is isotypical with that of voltaite and other cubic members of the group and their synthetic analogues (Table 9). The crystal structure of ammoniovoltaite consists of kröhnkite-like chains running along the diagonal between two crystallographic axes. These chains are built by alternating $M2X_6$ ($X_6 = O_4^{2-}$, $(H_2O)_2$ and $M1O_6$ octahedra linked *via* SO_4 tetrahedra (Fig. 8a). The *M*2 site is occupied

TABLE 2. Mössbauer parameters for ammoniovoltaite and its synthetic analogue.

	Γ (mm/s)	δ (mm/s)	ΔE_Q (mm/s)	%
Ammoniovoltaite $(NH_4)_2Fe^{2+}_5Fe^{3+}_3Al(SO_4)_{12}(H_2O)_{18}$ (this work)				
Fe^{2+}	0.372(6)	1.303(2)	1.856(4)	55.9
Fe^{3+}	0.398(9)	0.469(4)	0.311(0)	44.1
Synthetic $(NH_4)_2Fe^{2+}_5Fe^{3+}_3Al(SO_4)_{12}(H_2O)_{18}$ (Majzlan *et al.*, 2013)				
Fe^{2+}	0.338	1.312	1.819	63.3
Fe^{3+}	0.293	0.452	0.382	36.7

δ – isomer shift, ΔE_Q – quadrupole splitting, Γ – line width.

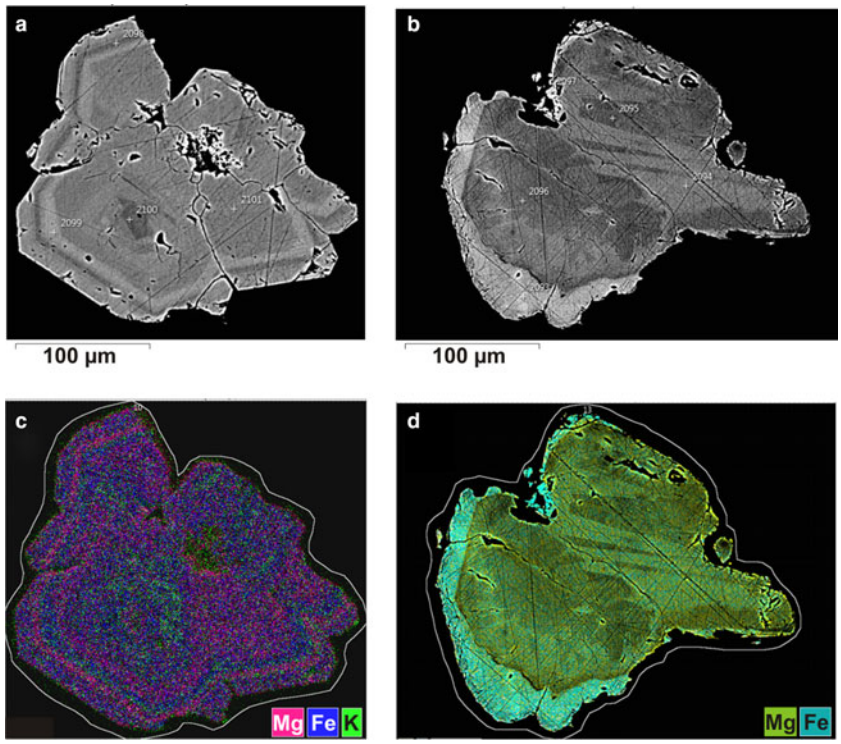

FIG. 7. (*a*, *b*) Back-scatter electron images of ammoniovoltaite crystals. Dark grey indicates Mg-rich zones and light grey correspond sto Fe-rich compositions (FeO 21.08–27.18 wt.%; MgO 0.69–3.72 wt.%). (*c*, *d*) False-colour element-distribution maps. Note the green colour in (*c*) designates regions enriched with K (0–0.27 wt.% K_2O).

TABLE 3. Chemical composition (in wt.%) of ammoniovoltaite.

Constituent	Mean	Range	Ideal[a]	Stand. Dev.	Probe standard
[FeO_{total}]	23.68	22.53–24.19	28.93	0.49	FeS_2
[FeO][b]	13.26		18.09		
[Fe_2O_3][b]	11.58		12.04		
MgO	2.33	1.65–3.26		0.08	MgO
ZnO	0.04	0.02–0.14		0.09	Zn
Al_2O_3	2.74	2.68–2.83	2.57	0.05	Al_2O_3
SO_3	47.46	47.08–47.66	48.36	0.39	$CaSO_4$
K_2O	0.19	0.07–0.30		0.02	KCl
CaO	0.11	0.11–0.13		0.02	$CaSO_4$
$(NH_4)_2O$[c]	2.96	2.11–3.75	2.62		BN
H_2O[d]	16.03				
Total	96.70		100.00		

[a]Calculated for the simplified formula $(NH_4)_2Fe^{2+}_5Fe^{3+}_3Al(SO_4)_{12}\cdot 18H_2O$.
[b]Distinguished by Mössbauer spectroscopy.
[c]Measured in EDS mode.
[d]Calculated from the crystal structure.

TABLE 4. Observed and calculated powder XRD data for ammoniovoltaite.

$2\theta_{meas}$ (°)	I_{meas}	d_{meas} (Å)	I_{calc}	d_{calc} (Å)	*h*	*k*	*l*
10.61	**74**	**9.67**	**8**	**9.67**	**0**	**2**	**2**
13.01	**56**	**7.90**	**9**	**7.90**	**2**	**2**	**2**
15.03	27	6.84	4	6.84	0	0	4
18.45	**84**	**5.58**	**26**	**5.58**	**4**	**2**	**2**
21.33	11	4.834	8	4.835	0	4	4
22.30	2	4.625	2	4.623	5	3	1
23.87	12	4.325	3	4.325	0	6	2
25.07	24	4.122	16	4.123	6	2	2
26.21	18	3.945	14	3.948	4	4	4
28.34	24	3.654	19	3.655	6	4	2
29.11	**100**	**3.560**	**94**	**3.561**	**7**	**3**	**1**
30.34	**100**	**3.418**	**100**	**3.419**	**0**	**0**	**8**
32.23	12	3.222	18	3.223	8	2	2
32.92	27	3.157	36	3.158	7	5	1
34.03	28	3.057	40	3.058	0	8	4
34.69	9	3.001	12	3.002	7	5	3
35.75	5	2.9145	6	2.9157	6	6	4
36.37	**37**	**2.8660**	**67**	**2.8672**	**9**	**3**	**1**
37.39	3	2.7904	3	2.7916	8	4	4
38.99	2	2.6807	3	2.6821	8	6	2
39.69	25	2.6350	16	2.6319	6	6	6
			6	2.6319	10	2	2
41.07	27	2.5500	40	2.5506	9	5	3
42.00	8	2.4961	17	2.4969	10	4	2
43.44	3	2.4169	11	2.4176	0	8	8
44.16	5	2.3794	3	2.3807	10	4	4
			8	2.3807	8	8	2
44.80	1	2.3471	2	2.3454	0	10	6
45.37	8	2.3191	13	2.3200	9	7	3
46.23	12	2.2785	23	2.2793	0	0	12
46.75	2	2.2547	9	2.2559	11	5	1
47.54	1	2.2194	2	2.2185	12	2	2
			2	2.2185	10	6	4
48.06	19	2.1966	19	2.1970	11	5	3
			31	2.1970	9	7	5
49.52	6	2.1356	7	2.1358	12	4	2
			10	2.1358	8	8	6
50.64	33	2.0914	98	2.0916	11	7	1
51.47	2	2.0602	6	2.0617	12	4	4
52.04	5	2.0392	3	2.0444	13	3	1
			4	2.0444	11	7	3
			11	2.0387	10	8	4
52.68	5	2.0159	21	2.0164	12	6	2
53.90	1	1.9736	2	1.9740	8	8	8
54.47	1	1.9548	1	1.9587	13	5	1
			1	1.9587	11	7	5
			4	1.9537	12	6	4
55.09	3	1.9342	15	1.9341	0	14	2
55.70	11	1.9148	33	1.9150	14	2	2
			1	1.9150	10	10	2
56.30	4	1.8959	14	1.8965	0	12	8
56.88	3	1.8783	17	1.8785	12	8	2
58.62	2	1.8273	13	1.8275	12	8	4

(continued)

TABLE 4. (*contd.*)

$2\theta_{meas}$ (°)	I_{meas}	d_{meas} (Å)	I_{calc}	d_{calc} (Å)	*h*	*k*	*l*
59.08	3	1.8142	13	1.8154	13	7	3
			4	1.8154	11	9	5
60.20	8	1.7836	35	1.7842	15	3	1
61.45	1	1.7507	6	1.7510	12	8	6
62.00	2	1.7367	10	1.7368	14	6	4
			8	1.7368	12	10	2
62.42	6	1.7262	19	1.7264	13	9	1
			8	1.7264	11	9	7
63.10	2	1.7094	5	1.7095	0	0	16
63.66	1	1.6962	5	1.6963	12	10	4
64.20	6	1.6833	24	1.6834	14	8	2
			13	1.6834	10	10	8
64.74	3	1.6707	27	1.6708	14	6	6
65.29	1	1.6583	3	1.6585	0	16	4
			7	1.6585	12	8	8
66.36	3	1.6345	17	1.6346	12	10	6
67.42	15	1.6117	90	1.6117	16	4	4
			7	1.6117	0	12	12
67.94	2	1.6008	24	1.6006	12	12	2
68.94	12	1.5805	27	1.5818	17	3	1
			8	1.5818	13	11	3
			9	1.5818	15	7	5
			5	1.5818	13	9	7
69.54	1	1.5685	10	1.5687	12	12	4
70.05	5	1.5585	4	1.5585	16	6	4
			24	1.5585	12	10	8
70.96	5	1.5411	29	1.5411	17	5	1
			8	1.5411	15	9	3
			9	1.5411	13	11	5
72.12	5	1.5196	20	1.5195	14	8	8
			8	1.5195	12	12	6
73.16	2	1.5009	6	1.5011	18	2	2
			19	1.5011	14	10	6
74.06	1	1.4854	12	1.4856	17	7	1
			4	1.4856	13	11	7
74.69	1	1.4746	16	1.4747	18	4	2
75.06	2	1.4684	19	1.4683	15	11	1
			6	1.4683	17	7	3

mainly by divalent cations, whereas the *M*1 site is preferable for trivalent cations. The three-dimensional arrangement of kröhnkite-like chains produces the framework (Hawthorne *et al*., 2000) shown in Fig. 8*b*. The framework contains two types of interstitial cavities: (1) those formed by $M2X_6$ octahedra and SO_4 tetrahedra and occupied by $(NH_4)^+$ molecules; and (2) those formed by $M1O_6$ octahedra and SO_4 tetrahedra and occupied by large $[Al(H_2O)_6]^{3+}$ complexes (Fig. 8). The following distances (values are given for data collected at 100 K) are observed for the first cavity-hosting ammonium ions: *A*–O3 = 3.317 Å and *A*–O4 = 2.900 Å. Therefore the coordination environments of the *A* site may be represented as a 12-vertex polyhedron with <*A*–O> = 3.108 Å and polyhedral volume ($V_{AlO_{12}}$) 72.2 Å^3. The cavity occupied by $Al(H_2O)_6$ complexes is formed by twelve O4 atoms with Al–O4 = 4.017 Å and $V_{AlO_{12}}$ = 157.3 Å^3 (Fig. 9). The NH_4 hosting cavities are arranged around $Al(H_2O)_6$-cavites in a tetrahedral manner.

From the data provided by Majzlan *et al*. (2013) it can be concluded that for K-dominant synthetic

TABLE 5. Crystallographic data, data collection information and refinement parameters for ammoniovoltaite.

Crystal data		
Crystal system	Cubic	
Space group	$Fd\bar{3}c$	
Unit-cell dimension a (Å)	27.250(1)	27.322(1)
Unit-cell volume (Å^3)	20234(2)	20396(3)
Z	16	16
Calculated density (g/cm^3)	2.549	2.529
Absorption coeff. (mm^{-1})	2.593	2.572
Data collection		
Diffractometer	Bruker APEX II DUO	Bruker APEX II DUO
Temperature (K)	100	293
Radiation, wavelength (Å)	Mo$K\alpha$, 0.71073	Mo$K\alpha$, 0.71073
θ range for data coll. (°)	2.11–32.27	2.11–34.50
h, k, l ranges	$-34 \le h \le 11$	$-26 \le h \le 42$
	$-14 \le k \le 40$	$-29 \le k \le 22$
	$-33 \le l \le 30$	$-43 \le l \le 22$
Axis, frame width (°), time per frame (s)	ω, 0.5, 40	ω, 0.5, 45
Reflections collected	8816	11150
Unique refl. (R_{int})	1509 (0.041)	1814 (0.039)
Unique refl. $F > 2\sigma(F)$	1217	1462
Data completeness to θ_{max} (%)	99.5	99.7
Structure refinement		
Refinement method	Full-matrix least-squares on F^2	
Weighting coeff. a, b	0.060000, 0.500000	0.060000, 0.500000
Data/restrains/parameters	1509/2/95	1814/2/95
R_1 [$F > 4\sigma(F)$], wR_2 [$F > 4\sigma(F)$]	0.031, 0.086	0.030, 0.084
R_1 all, wR_2 all	0.044, 0.093	0.043, 0.091
Goodness-of-fit on F^2	0.999	1.000
Largest diff. peak and hole (e^-Å^{-3})	1.06, –0.48	1.09, –0.40

voltaites, the <*A*–O> ranges within 3.02–3.08 Å with the highest value attributed to K-Fe species, whereas for NH_4-dominant voltaites the <*A*–O> is slightly longer being 3.11 and 3.10 Å for NH_4-Fe and NH_4-Mn forms, respectively. In ammoniovoltaite <*A*–O> is 3.11 at 100 K and 3.12 at RT that suggests that the <*A*–O> distance may be a useful sign of occupancy of the *A* site in voltaites.

The observed <S^{6+}–O> distances (Table 8) are 1.472 Å (at 100 K) and 1.470 Å (at RT) and fall within the range reported for synthetic voltaites: 1.470–1.475 Å (Majzlan *et al*., 2013). The range of <Al–O> distances for synthetic voltaites is 1.83–1.87 Å (Majzlan *et al*., 2013) and our values [1.880 Å (at 100 K) and 1.874 (at RT), Table 8] are very similar. The <*M*2–*X*> distance shows broad variations in synthetic voltaites (2.03–2.17 Å) depending on the radii of the dominant divalent cation (Majzlan *et al*., 2013). However, the values of <*M*2–*X*> obtained in our study coincides with the value reported for NH_4-Fe voltaite (Majzlan *et al*., 2013) despite the fact that the occupancy of *M*2 site is different for the two (Fe in the synthetic and Fe, Mg in the natural sample). No direct correlation is observed between <*M*1–O> and occupancy of the *M*1 site as reported in the series *M*1 = Fe^{3+} studied by Majzlan *et al*. (2013), but <*M*1–O> varies in the range 1.97–2.08 Å. The NH_4-Fe sample is reported with <*M*1–O> = 1.97 Å, while our value is slightly larger, 2.00 Å (Table 8).

Discussion

Ammoniovoltaite is a new member of the voltaite group (Table 9), and is the NH_4-analogue of voltaite and the Fe^{2+}-dominant analogue of ammoniomagnesiovoltaite. It is also the first ammonium-dominant voltaite-group mineral with a determined crystal structure. The synthetic analogue of

TABLE 6. Atom coordinates, site occupancies and equivalent isotropic displacement parameters (Å^2) for ammoniovoltaite.

Site	*T*, K	Wyckoff symbol	Composition[1]	s.s.[2]	calc. s.s.[3]	*x*	*y*	*z*	$U_{eq/iso}$
A	100	32*b*	$N_{0.94}K_{0.04}Ca_{0.02}$	8.28(4)	7.74	¼	¼	¼	0.0246(4)
	293			8.33(3)		¼	¼	¼	0.0264(3)
*M*1	100	32*c*	$Fe^{3+}_{0.97}Al_{0.03}$	25.54(3)	25.61	0	0	0	0.00645(5)
	293			25.65(2)		0	0	0	0.01122(4)
*M*2	100	96*g*	$Fe^{2+}_{0.62}Mg_{0.20}$	23.04(2)	23.24	¼	0.10223(2)	−0.10223(2)	0.00792(4)
	293		$Fe^{3+}_{0.17}Zn_{0.01}$	22.27(1)		¼	0.10280(2)	−0.10280(2)	0.01328(3)
Al	100	16*a*	Al			⅛	⅛	⅛	0.0064(2)
	293					⅛	⅛	⅛	0.0106(1)
S	100	192*h*	S			0.23680(2)	0.27613(2)	0.11758(2)	0.00791(4)
	293					0.23739(2)	0.27570(2)	0.11765(2)	0.01231(3)
O1	100	192*h*	O			0.24946(2)	0.24712(2)	0.07342(2)	0.0113(1)
	293					0.24968(2)	0.24709(2)	0.07326(2)	0.0183(1)
O2	100	192*h*	O			0.22342(3)	0.32653(2)	0.10344(2)	0.0160(2)
	293					0.22394(2)	0.32606(2)	0.10396(2)	0.0242(1)
O3	100	192*h*	O			0.19424(2)	0.25405(2)	0.14189(2)	0.0188(2)
	293					0.19537(2)	0.25355(2)	0.14207(2)	0.0301(2)
O4	100	192*h*	O			0.27910(2)	0.27640(2)	0.15108(2)	0.0145(1)
	293					0.27986(2)	0.27595(2)	0.15057(2)	0.0235(1)
$O5_w$	100	192*h*	H_2O			0.18076(2)	0.42239(2)	0.12157(2)	0.0164(2)
	293					0.18079(2)	0.42199(2)	0.12183(2)	0.0272(1)
$O6_w$	100	192*h*	$□_{0.75}(H_2O)_{0.25}$			0.0819(9)	0.14723(8)	0.07093(8)	0.0140(6)
	293					0.08981(8)	0.14703(7)	0.07115(7)	0.0213(5)
$O7_w$	100	192*h*	$□_{0.75}(H_2O)_{0.25}$			0.08897(9)	0.10366(8)	0.06965(9)	0.0154(6)
	293					0.08985(8)	0.10352(7)	0.06940(8)	0.0241(5)
H1	100	192*h*				0.1809(8)	0.4304(7)	0.1542(5)	0.114(7)
	293					0.1867(8)	0.4349(7)	0.1544(5)	0.174(9)
H2	100	192*h*				0.1726(5)	0.4469(4)	0.1001(4)	0.051(4)
	293					0.1697(5)	0.4444(4)	0.0972(5)	0.096(5)

[1]In agreement with the formula obtained by microprobe and Mössbauer data, $[(NH_4)_{1.88}K_{0.08}Ca_{0.04}]_{\Sigma 2.00}(Fe^{2+}_{3.74}Mg_{1.17}Fe^{3+}_{0.05}Zn_{0.01})_{\Sigma 4.97}(Fe^{3+}_{2.89}Al_{0.09})_{\Sigma 2.98}Al_{1.00}(SO_4)_{12.00}(H_2O)_{18.00}$; [2]Site scattering in electrons per formula unit; [3] Calculated site scattering in electrons per formula unit.

TABLE 7. Anisotropic displacement parameters (Å^2) of atoms in the structure of ammoniovoltaite.

Atom	*T*, K	U^{11}	U^{22}	U^{33}	U^{23}	U^{13}	U^{12}
N	100	0.0246(4)	0.0246(4)	0.0246(4)	0.0059(4)	0.0059(4)	0.0059(4)
	293	0.0264(3)	0.0264(3)	0.0264(3)	0.0099(3)	0.0099(3)	0.0099(3)
*M*1	100	0.00649(5)	0.00649(5)	0.00649(5)	0.00160(6)	0.00160(6)	0.00160(6)
	293	0.01122(4)	0.01122(4)	0.01122(4)	0.00219(4)	0.00219(4)	0.00219(4)
*M*2	100	0.00806(7)	0.00786(4)	0.00786(4)	−0.00050(6)	−0.00011(5)	−0.00011(5)
	293	0.01428(6)	0.01278(4)	0.01278(4)	−0.00097(5)	−0.00038(4)	−0.00038(4)
Al	100	0.0064(2)	0.0064(2)	0.0064(2)	0.00000	0.00000	0.00000
	293	0.0106(1)	0.0106(1)	0.0106(1)	0.00000	0.00000	0.00000
S	100	0.00879(7)	0.00766(7)	0.00728(7)	−0.00010(6)	0.00056(7)	−0.00024(7)
	293	0.01349(6)	0.01181(5)	0.01163(6)	−0.00020(5)	0.00038(5)	−0.00077(5)
O1	100	0.0133(2)	0.0123(2)	0.0083(2)	−0.0021(2)	−0.0013(2)	0.0034(2)
	293	0.0232(2)	0.0194(2)	0.0124(2)	−0.0033(2)	−0.0024(2)	0.0037(2)
O2	100	0.0243(3)	0.0089(2)	0.0150(3)	0.0010(2)	0.0009(2)	0.0022(2)
	293	0.0357(3)	0.0134(2)	0.0236(2)	0.0009(2)	−0.0005(2)	0.0029(2)
O3	100	0.0166(3)	0.0195(3)	0.0204(3)	0.0014(3)	0.0078(2)	−0.0066(2)
	293	0.0279(2)	0.0302(3)	0.0322(3)	0.0011(2)	0.0123(2)	−0.0103(2)
O4	100	0.0141(3)	0.0211(3)	0.0083(2)	−0.0053(2)	−0.0022(2)	0.0016(2)
	293	0.0202(2)	0.0353(3)	0.0151(2)	−0.0068(2)	−0.0034(2)	0.0046(2)
$O5_w$	100	0.0127(2)	0.0220(3)	0.0145(3)	−0.0022(2)	0.0010(2)	0.0020(2)
	293	0.0203(2)	0.0368(3)	0.0246(2)	−0.0021(2)	0.0024(2)	0.0050(2)
$O6_w$	100	0.012(1)	0.018(1)	0.012(1)	0.003(1)	−0.006(9)	−0.003(9)
	293	0.0229(9)	0.0265(9)	0.0146(8)	0.0091(7)	−0.0068(8)	−0.0046(8)
$O7_w$	100	0.016(1)	0.014(1)	0.016(1)	−0.005(1)	−0.007(1)	0.0027(9)
	293	0.0218(9)	0.029(1)	0.0217(8)	−0.0101(8)	−0.0107(8)	0.0052(8)

TABLE 8. Selected bond lengths (Å) in the structure of ammoniovoltaite.

	T = 100 K	*T* = 293 K
*M*1–O1	2.0021(6) × 6	2.0033(5) × 6
<*M*1–O>	2.002	2.003
*M*2–$O5_w$	2.0706(6) × 2	2.0747(5) × 2
*M*2–O2	2.0722(6) × 2	2.0704(6) × 2
*M*2–O4	2.1205(6) × 2	2.1173(6) × 2
<*M*2–*X*>	2.088	2.087
S–O3	1.4648(7)	1.4595(6)
S–O4	1.4704(6)	1.4681(5)
S–O2	1.4723(7)	1.4724(6)
S–O1	1.4807(6)	1.4813(5)
<S–O>	1.472	1.470
Al–$O6_w$	1.868(2) × 12	1.858(2) × 12
Al–$O7_w$	1.891(2) × 12	1.890(2) × 12
<Al–O>	1.880	1.874

ammoniovoltaite was previously obtained and studied by Sajó (2012) and Majzlan *et al*. (2013). Previous comprehensive studies of synthetic voltaites (Beveridge and Day, 1979; Gossner and Bäuerlein, 1930, 1933; Gossner and Fell, 1932; Gossner and Besslein, 1934; Majzlan *et al*., 2013) showed evidence for incorporation into the voltaite-type structure of a number of different divalent M^{2+} cations (M^{2+} = Fe, Mg, Zn, Cd, Co and Mn) in comparison to the natural members (M^{2+} = Fe, Mg and Zn). The *A* site is populated in natural species either by NH_4^+ or K^+ with minor contents of other alkali and alkali-earth metals such as Na and Ca, whereas synthetic samples were also obtained with Tl^+ and Rb^+ (Gossner and Fell, 1932; Gossner and Besslein, 1934).

The ammonium ion is characteristic of specific geological conditions. Ammoniovoltaite was discovered at a geothermal field characterized by a high ammonium concentration. Another $(NH_4)^+$ member of the voltaite group, ammoniomagnesiovoltaite, was found in a burning coal dump (Szakáll

TABLE 9. Comparative data for ammoniovoltaite, its synthetic analogue and voltaite-group minerals.

Mineral/ compound	Ammoniovoltatite	Synthetic analogue*	Ammonio-magnesiovoltaite	Voltaite	Zincovoltaite	Magnesiovoltaite	Pertlikite
Chemical formula	$(NH_4)_2Fe^{2+}_5Fe^{3+}_3Al(SO_4)_{12}(H_2O)_{18}$		$(NH_4)_2Mg_5Fe^{3+}_3Al(SO_4)_{12}(H_2O)_{18}$	$K_2Fe^{2+}_5Fe^{3+}_3Al(SO_4)_{12}(H_2O)_{18}$	$K_2Zn^{2+}_5Fe^{3+}_3Al(SO_4)_{12}(H_2O)_{18}$	$K_2Mg^{2+}_5Fe^{3+}_3Al(SO_4)_{12}(H_2O)_{18}$	$K_2(Fe^{2+},Mg)_2Mg_4Fe^{3+}_2Al(SO_4)_{12}(H_2O)_{18}$
Crystal system				Cubic			Tetragonal
Space group				$Fd\bar{3}c$			$I4_1/acd$
a, Å	27.322(1)[a]	27.239(3)[b]	27.260(2)	27.254(8)	27.180(1)	27.161(1)	19.2080(3)
c, Å	= a	= a	= a	= a	= a	= a	27.2158(7)
V, Å^3	20234(2)	20210(4)	20257(2)	20244	20079.29	20038(2)	10041.2(6)
R_1 (%)	0.030	0.022	No single-crystal data	0.033	n.a.	0.032	0.022
Strongest lines of the powder X-ray diffraction pattern: d, Å (I, %)	9.67 (74), 7.90 (56), 5.58 (84), 3.560 (100), 3.418 (100), 2.8660 (37)	9.63 (54),[c] 7.86 (15), 5.56 (100), 3.546 (32), 3.405 (28), 2.855 (15)	6.85 (24), 5.59 (100), 3.420 (72), 3.562 (66), 1.7836 (25), 1.5582 (25)	9.64 (64), 6.81 (30) 5.56 (69), 3.548 (81), 3.407 (100), 2.8570 (35)	5.53 (48), 4.24 (28), 3.54 (67), 3.39 (100), 3.13 (39), 2.84 (32)	6.77 (37), 5.53 (61), 3.532 (68), 3.392 (100), 3.034 (45), 2.845 (30)	5.543 (28), 3.396 (100), 3.136 (21), 3.038 (39), 2.848 (31), 2.078 (29),
D_{calc} /D_{meas} (g/cm^{-3})	2.529/n.a.	2.585/n.a.	2.351/n.a.	2.663/n.a.	2.767/2.756	2.506/2.51(2)	2.56(1)/2.59(3)
Reference	This proposal	Majzlan *et al.* (2013)	Szakáll *et al.* (2012)	Mereiter (1972)	Li *et al.* (1987)	Chukanov *et al.* (2016)	Ertl *et al.* (2008)

*Synthetic analogue of ammoniovoltatite (NH_4-Fe).
[a]RT value, a = 27.250(1) at 100 K; [b]at 120 K; [c]calculated using the cif (ICSD 188360).
n.a. – not analysed or not available.

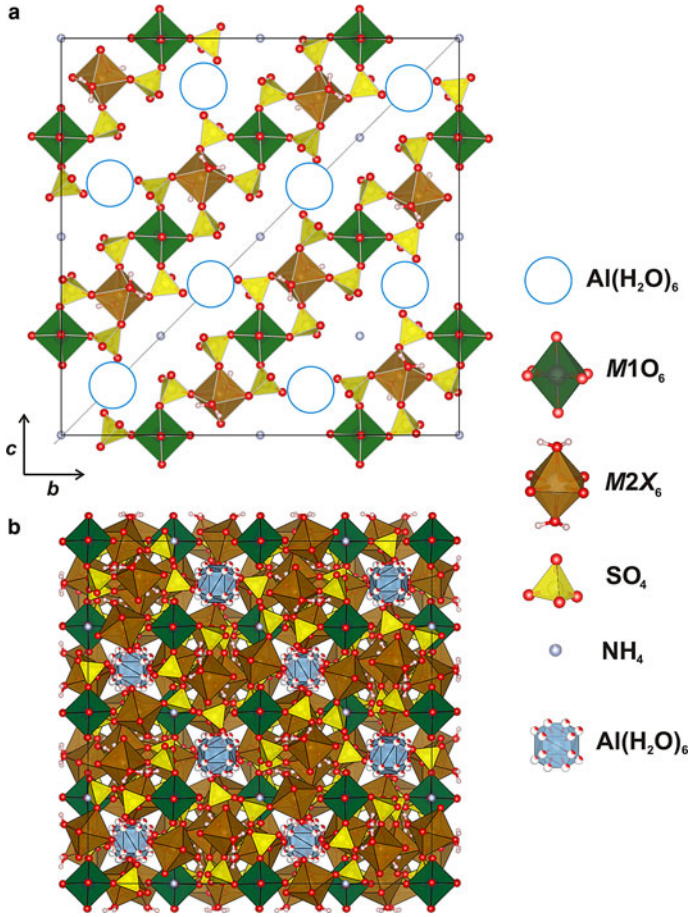

FIG. 8. (*a*) General projection of the crystal structure of ammoniovoltaite. Kröhnkite-type chains are highlighted and Al$(H_2O)_6$ groups are omitted (designated by blue circles) for clarity. (*b*) Three-dimensional framework of ammoniovoltaite.

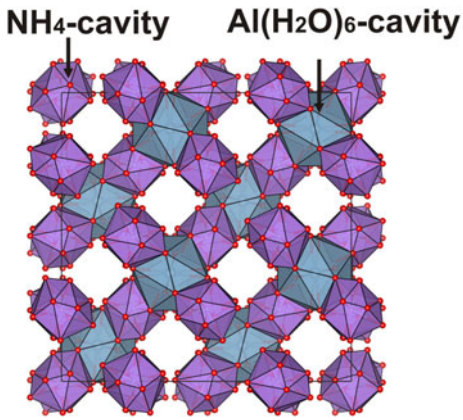

FIG. 9. Three-dimensional arrangement of NH_4- (purple) and Al$(H_2O)_6$ (grey) hosting cavities in the crystal structure of ammoniovoltaite.

et al., 2012). The question of ammonium sources and distribution of ammonium minerals are worth a more detailed discussion. The current IMA list contains 67 ammonium minerals (mostly sulfates) out of 5224 approved mineral species. The majority of these minerals originates from: (1) volcanic activity (~29%) (Table 10); (2) guano decomposition (~25%) [e.g. möhnite (Chukanov *et al*., 2015), niahite (Bridge and Robinson, 1983) and struvite (Maclvor, 1887; Yang *et al*., 2014)]; and (3) black lignitic shales, burning coal seams or natural fires in oil-bearing shale (19%) [e.g. ammoniomagnesiovoltaite (Szakáll *et al*., 2012), carlsonite and huizingite-(Al) (Kampf *et al*., 2016)].

Regarding volcanically active geological environments, ammonium minerals are reported at: (1) fumaroles of active volcano cones; (2) gas/steam

TABLE 10. List of volcanogenic ammonium minerals.

Mineral	Chemical formula from IMA list 2017	Type locality (or localities of later findings*)	Reference
Active volcano cones (implies the presence of the volcano's feeding channel)			
Adranosite	$(NH_4)_4NaAl_2(SO_4)_4Cl(OH)_2$	La Fossa crater, Vulcano Island, Sicily, Italy	Demartin *et al.* (2010*a*)
Adranosite-(Fe)	$(NH_4)_4NaFe_2(SO_4)_4Cl(OH)_2$	La Fossa crater, Vulcano Island, Sicily, Italy	Mitolo *et al.* (2013)
Aluminopyracmonite	$(NH_4)_3Al(SO_4)_3$	La Fossa crater, Vulcano Island, Sicily, Italy	Demartin *et al.* (2013)
Argesite	$(NH_4)_7Bi_3Cl_{16}$	La Fossa crater, Vulcano Island, Sicily, Italy	Demartin *et al.* (2012)
Bararite	$(NH_4)_2SiF_6$	Mt Vesuvius, Naples Province, Campania, Italy*	Palache *et al.* (1951)
Barberiite	$(NH_4)BF_4$	La Fossa crater, Vulcano Island, Sicily, Italy	Garavelli and Vurro (1994)
Brontesite	$(NH_4)_3PbCl_5$	La Fossa crater, Vulcano Island, Sicily, Italy	Demartin *et al.* (2009*a*)
Campostriniite	$(Bi_{2.5}Na_{0.5})(NH_4)_2Na_2(SO_4)_6\cdot H_2O$	La Fossa crater, Vulcano Island, Sicily, Italy	Demartin *et al.* (2015)
Cryptohalite	$(NH_4)_2SiF_6$	Mt Vesuvius, Naples Province, Campania, Italy	Scacchi (1873)
Lucabindiite	$(K,NH_4)As_4O_6(Cl,Br)$	La Fossa crater, Vulcano Island, Sicily, Italy	Garavelli *et al.* (2013)
Kremersite	$(NH_4)_2Fe^{3+}Cl_5\cdot H_2O$	Mt Vesuvius, Naples Province, Campania, Italy*	Palache *et al.* (1951)
Panichiite	$(NH_4)_2SnCl_6$	La Fossa crater, Vulcano Island, Sicily, Italy	Demartin *et al.* (2009*b*)
Pyracmonite	$(NH_4)_3Fe(SO_4)_3$	La Fossa crater, Vulcano Island, Sicily, Italy	Demartin *et al.* (2010*b*)
Therasiaite	$(NH_4)_3KNa_2Fe^{2+}Fe^{3+}(SO_4)_3Cl_5$	La Fossa crater, Vulcano Island, Sicily, Italy	Demartin *et al.* (2014)
Thermessaite-(NH_4)	$(NH_4)_2AlF_3(SO_4)$	La Fossa crater, Vulcano Island, Sicily, Italy	Garavelli *et al.* (2012)
Geothermal fields (implies the presence of a deep source of heat and hydrothermal activity)			
Ammonioalunite	$(NH_4)Al_3(SO_4)_2(OH)_6$	Geysers, California, USA*	Dunning and Cooper (1993)
Ammonioborite	$(NH_4)_3B_{15}O_{20}(OH)_8\cdot 4H_2O$	Larderello, Pisa Province, Tuscany, Italy	Schaller (1933)
Ammoniojarosite	$(NH_4)Fe_3^{3+}(SO_4)_2(OH)_6$	Geysers, California, USA*	Dunning and Cooper (1993)
Ammoniovoltaite	$(NH_4)_2Fe_5^{2+}Fe_3^{3+}Al(SO_4)_{12}(H_2O)_{18}$	Severo-Kambalny geothermal field, Southern Kamchatka, Russia	This work
Boussingaultite	$(NH_4)_2Mg(SO_4)_2\cdot 6H_2O$	Travale, Montieri, Grosseto Province, Tuscany, Italy	Bechi (1864)
		Geysers, California, USA*	Dunning and Cooper (1993)
Larderellite	$(NH_4)B_5O_7(OH)_2\cdot H_2O$	Larderello, Pisa Province, Tuscany, Italy	Bechi (1854)
Letovicite	$(NH_4)_3H(SO_4)_2$	Geysers, California, USA*	Dunning and Cooper (1993)
Mascagnite	$(NH_4)_2(SO_4)$	Travale, Montieri, Grosseto Province, Tuscany, Italy	Mascagni (1779)
		Geysers, California, USA*	Dunning and Cooper (1993)
Mohrite	$(NH_4)_2Fe^{2+}(SO_4)_2\cdot 6H_2O$	Travale, Montieri, Grosseto Province, Tuscany, Italy	Garavelli (1964)
Tschermigite	$(NH_4)Al(SO_4)_2\cdot 12H_2O$	Geysers, California, USA*	Dunning and Cooper (1993)

vents and/or efflorescence areas at geothermal fields and (3) the surface of fresh lava flows.

Active volcano cones

The locality with the largest reported number of ammonium minerals to date is La Fossa crater, Vulcano, Aeolian Islands, Sicily, Italy (Campostrini *et al*., 2011), which is an active volcano cone and type locality of seven ammonium sulfates and five ammonium halides (Table 10). Ammonium minerals at La Fossa crater are reported as sublimates around fumaroles formed at temperatures of ~170–350°C (e.g. argesite, lucabindiite and pyracmonite). Another example of an active volcano cone where ammonium mineralization has been reported is Mt Vesuvius, Naples Province, Campania, Italy.

Lava flows

Sal ammoniac (NH_4Cl) is a relatively abundant natural phase occurring at the surface of the fresh lava flows (e.g. Tolbachik eruptions; Fedotov and Markhinin, 1983).

Geothermal fields

Until recently, most of the ammonium minerals first discovered at geothermal fields were reported from the Larderello–Travalle geothermal province (Table 10) and first described before 1911 (the time when the first geothermal power plant was built). Ammonium mineralization is also reported from the Geysers geothermal system, California, USA (Dunning and Cooper, 1993) and a number of other localities in California, USA (Krohn *et al*., 1993) (Table 10).

For geothermal fields located in Southern Kamchatka (Fig. 1) two potential sources of nitrogen are discussed: (1) deep magmatic or/and (2) biogenic from underlying sedimentary rocks containing organic material. The isotope study performed on ammonium minerals including geothermal fields at Kambalny volcanic ridge (Volynets *et al*., 1967) provided a broad range of δN^{15} (= ^{15}N:^{14}N) that did not allow the source of N to be established for certain. The nitrogen source for Southern Kamchatka geothermal fields associated with Kambalny and Koshelev volcanos remains unclear at present and requires additional isotope studies.

Acknowledgements

We are grateful to Uwe Kolitsch, Nikita V. Chukanov and Peter Leverett for very helpful comments on the manuscript. This study was supported by the Russian Foundation of Basic Research, 16-05-00007 (field works and part of the study) and Russian Science Foundation, 16-17-10085 (structural studies). We thank Dr. Alexey Goncharov (Dept. Geochemistry, SPbSU) for collecting and interpretation of Mössbauer spectra. The technical support by the SPbSU X-Ray Diffraction and Geomodel Research Resource Centers is gratefully acknowledged.

Supplementary material

To view supplementary material for this article, please visit https://doi.org/10.1180/minmag.2017.081.083

References

Bechi, E. (1854) Analysis of several native borates: larderellite, (new species). *American Journal of Science*, **67**, 129–130.

Beveridge, D. and Day, P. (1979) Charge transfer in mixed valence solids. Part 9. Preparation, characterization, and optical spectroscopy of the mixed valence mineral voltaite [aluminum pentairon(II) triiron(III) dipotassium dodecasulfate 18-hydrate] and its solid solutions with cadmium(II). *Journal of the Chemical Society, Dalton Transactions*, **10**, 648–653.

Bridge, P.J. and Robinson, B.W. (1983) Niahite – a new mineral from Malaysia. *Mineralogical Magazine*, **47**, 79–80.

Britvin, S.N., Dolivo-Dobrovolsky, D.V. and Krzhizhanovskaya, M.G. (2017) Software for processing of X-ray powder diffraction data obtained from the curved image plate detector of Rigaku RAXIS Rapid II diffractometer. *Zapiski Rossiiskogo Mineralogicheskogo Obshchetstva*, **CXLVI**, 104–107 [in Russian with English abstract].

Bruker-AXS (2014) *APEX2*. Version 2014.11–0. Madison, Wisconsin, USA

Bruker-AXS (2009) *Topas V4.2: General Profile and Structure Analysis Software for Powder Diffraction Data*. Karlsruhe, Germany.

Campostrini, I., Demartin, F., Gramaccioli, C.M. and Russo, M. (2011) *Vulcano – Tre secoli di mineralogia*. Associazione Micro-mineralogica Italiana, Cremona, 344 pp. [in Italian].

Chukanov, N.V. (2014) *Infrared Spectra of Mineral Species: Extended Library*. Springer-Verlag GmbH, Dordrecht-Heilderberg-New York-London, 1726 pp.

Chukanov, N.V., Aksenov, S.M., Rastsvetaeva, R.K., Pekov, I.V., Belakovskiy, D.I. and Britvin, S.N. (2015)

Möhnite, $(NH_4)K_2Na(SO_4)_2$, a new guano mineral from Pabellon de Pica, Chile. *Mineralogy and Petrology*, **109**, 643–648.

Chukanov, N.V., Aksenov, S.M., Rastsvetaeva, R.K., Möhn, G., Rusakov, V.S., Pekov, I.V., Scholz, R., Eremina, T.A., Belakovskiy, D.I. and Lorenz, J.A. (2016) Magnesiovoltaite, $K_2Mg_5^{2+}Fe_3^{3+}Al[SO_4]_{12}\cdot 18H_2O$, a new mineral from the Alcaparrosa mine, Antofagasta region, Chile. *European Journal on Mineralogy*, **28**, 1005–10017.

Demartin, F., Castellano, C. and Campostrini, I. (2013) Aluminopyracmonite, $(NH_4)_3Al(SO_4)_3$, a new ammonium aluminium sulfate from La Fossa crater, Vulcano, Aeolian Islands, Italy. *Mineralogical Magazine*, **77**, 443–451.

Demartin, F., Gramaccioli, C.M. and Campostrini, I. (2009*a*) Brontesite, $(NH_4)_3PbCl_5$, a new product of fumarolic activity from La Fossa crater, Vulcano, Aeolian Islands, Italy. *The Canadian Mineralogist*, **47**, 1237–1243.

Demartin, F., Campostrini, I. and Gramaccioli, C.M. (2009*b*) Panichiite, natural ammonium hexachlorostannate(IV), $(NH_4)_2SnCl_6$, from La Fossa crater, Vulcano, Aeolian Islands, Italy. *The Canadian Mineralogist*, **47**, 367–372.

Demartin, F., Gramaccioli, C.M. and Campostrini, I. (2010*a*) Adranosite, $(NH_4)_4NaAl_2(SO_4)_4Cl(OH)_2$, a new ammonium sulfate chloride from La Fossa Crater, Vulcano, Aeolian Islands, Italy. *The Canadian Mineralogist*, **48**, 315–321.

Demartin, F., Gramaccioli, C.M. and Campostrini, I. (2010*b*) Pyracmonite, $(NH_4)_3Fe(SO_4)_3$, a new ammonium iron sulfate from La Fossa crater, Vulcano, Aeolian Islands, Italy. *The Canadian Mineralogist*, **48**, 307–313.

Demartin, F., Campostrini, I., Castellano, C. and Gramaccioli, C.M. (2012) Argesite, $(NH_4)_7Bi_3Cl_{16}$, a new mineral from La Fossa Crater, Vulcano, Aeolian Islands, Italy: A first example of the $[Bi_2Cl_{10}]^{4-}$ anion. *American Mineralogist*, **97**, 1446–1451.

Demartin, F., Castellano, C. and Campostrini, I. (2014) Therasiaite, $(NH_4)_3KNa_2Fe^{2+}Fe^{3+}(SO_4)_3Cl_5$, a new sulfate chloride from La Fossa Crater, Vulcano, Aeolian islands, Italy. *Mineralogical Magazine*, **78**, 203–213.

Demartin, F., Castellano, C. and Gramaccioli, C.M. (2015) Campostriniite, $(Bi^{3+},Na)_3(NH_4,K)_2Na_2(SO_4)_6\cdot H_2O$, a new sulfate isostructural with görgeyite, from La Fossa Crater, Vulcano, Aeolian Islands, Itlay. *Mineralogical Magazine*, **79**, 1007–1018.

Dunning, G.E. and Cooper, J.F. (1993) History and minerals of the Geysers Sonoma County, California. *The Mineralogical Records*, **24**, 339–354.

Ertl, A., Dyar, M.D., Hughes, J.M., Brandstätter, F., Gunter, M.E. and Prem, M. (2008) Pertlikite, a new tetragonal Mg-rich member of voltaite group from Madeni Zakh, Iran. *The Canadian Mineralogist*, **46**, 661–669.

Fedotov, S.A. and Markhinin, Ye.K. (editors) (1983) *The Great Tolbachik Fissure Eruption: geological and geophysical data 1975–1976. Cambridge*. Cambridge University Press, Cambridge, UK.

Gangé, O.C. and Hawthorne, F.C. (2015) Comprehensive derivation of bond-valence parameters for ion pairs involving oxygen. *Acta Crystallographica*, **B71**, 562–578.

Garavelli, C.L. (1964) Mohrite: un nuovo minerale della zona borifera toscana. *Atti della Accademia Nazionale dei Lincei. Rendiconti della Classe di Scienze Fisiche, Matematiche e Naturali*, **36**, 524–533.

Garavelli, A. and Vurro, F. (1994) Barberiite, NH_4BF_4, a new mineral from Vulcano, Aeolian Islands, Italy. *American Mineralogist*, **79**, 381–384.

Garavelli, A., Mitolo, D. and Pinto, D. (2012) Thermessaite-(NH_4), IMA 2011-077. CNMNC Newsletter No. 12, February 2012. *Mineralogical Magazine*, **76**, 152.

Garavelli, A., Mitolo, D., Pinto, D. and Vurro, F. (2013) Lucabindiite, $(K,NH_4)As_4O_6(Cl,Br)$, a new fumarole mineral from the "La Fossa" crater at Vulcano, Aeolian Islands, Italy. *American Mineralogist*, **98**, 470–477.

Gossner, B. and Bäuerlein, T. (1930) Hydrated sulfates containing three metals. *Berichte der Deutschen Chemischen Gesellschaft*, **63B**, 2151–2155.

Gossner, B. and Bauerlein, T. (1933) Optical anomalies: voltaite-like sulfates. *Neues Jahrbuch für Geologie and Paläontologie*, **66A**, 1–40.

Gossner, B. and Besslein, J. (1934) Hydrated sulfates of three metals. *Centralblatt für Mineralogie, Geologie und Paleontologie*, **1934A**, 358–364.

Gossner, B. and Fell, E. (1932) Sulfates of the voltaite type. Berichte der Deutschen Chemischen Gesellschaft, **65B**, 393–395.

Hawthorne, F.C., Krivovichev, S.V. and Burns, P.C. (2000) The crystal chemistry of sulfate minerals. Pp. 1–112 in: *Sulfate Minerals: Crystallography, Geochemistry, and Environmental Significance* (C.N. Alpers, J.L. Jambor and D.K. Nordstrom, editors). Reviews in Mineralogy & Geochemistry, **40**. The Mineralogical Society of America and the Geochemical Society, Washington DC.

Kalacheva, E.G., Rychagov, S.N., Nuzhdaev, A.A. and Koroleva, G.P. (2016) The geochemistry of steam hydrothermal occurences in the Koshelev volcanic massif, southern Kamchatka. *Journal of Volcanology and Seismology*, **10**, 188–202.

Kampf, A.R., Richards, R.P., Nash, B.P., Murowchick, J. B., Rakovan, J.F. (2016) Carlsonite, $(NH_4)_5Fe_3^{3+}O(SO_4)_6\cdot 7H_2O$, and huizingite-(Al), $(NH_4)_9Al_3(SO_4)_8(OH)_2\cdot 4H_2O$, two new minerals from a natural fire in an oil-bearing shale near Milan, Ohio. *American Mineralogist*, **101**, 2095–2107.

Krohn, M.D., Kendall, C., Evans, J.R. and Fries, T.L. (1993) Relations of ammonium minerals at several hydrothermal systems in the western U.S. *Journal of Volcanology and Geothermal Research*, **56**, 401–403.

Li, W., Chen, G. and Sun, S. (1987) Zincovoltaite – a new sulphate mineral. *Acta Mineralogica Sinica*, **7**, 307–321.

MacIvor, R.W.E. (1887) On Australian bat guano and some minerals occurring therein. *The Chemical News*, **55**, 215–216.

Majzlan, J., Schlicht, H., Wierzbicka-Wieczorek, M., Giester, G., Pöllmann, H., Brömme, B., Doyle, S., Buth, G. and Koch, C.B. (2013) A contribution to the crystal chemistry of the voltaite group: solid solutions, Mössbauer and infrared spectra, and anomalous anisotropy. *Mineralogy and Petrology*, **107**, 221–233.

Mandarino, J.A. (2007) The Gladstone–Dale compatibility of minerals and its use in selecting mineral species for further study. *The Canadian Mineralogist*, **45**, 1307–1324.

Mascagni, P. (1779) *Dei lagoni del senese e del volterrano*. Sienna, Italy.

Mereiter, K. (1972) Die Kristallstruktur des Voltaits, $K_2Fe_5^{2+}Fe_3^{3+}Al[SO_4]_{12}\cdot 18H_2O$. *Tschermaks Mineralogische Petrographische Mitteilungen*, 18, 185–202 [in German].

Mitolo, D., Demartin, F., Garavelli, A., Campostrini, I., Pinto, D., Gramaccioli, C.M., Acquafredda, P. and Kolitsch, U. (2013) Adranosite-(Fe), $(NH_4)_4NaFe_2(SO_4)_4Cl(OH)_2$, a new ammonium sulfate chloride from La Fossa Crater, Vulcano, Aeolian Islands, Italy. *The Canadian Mineralogist*, **51**, 57–66.

Nekhoroschev, A.S. (1959) Hydrothermal activity of Kambalny ridge, Southern Kamchatka. *Bulletin of Vulcanological station*, **28**, 23–33 [in Russian].

Ogorodova, A.S., Naboko, S.I., Fedotov, S.A. and Vinogradov, V.N. (1971) *Trace elements in modern hydrothermally-altered rocks and minerals on the example of hydrothermal field (Yuzhno-Kambalny and Pauzhetskaya geothermal systems)*. Report of the Institute of Volcanology (Far-eastern branch of the USSR Academy of Sciences), Department of Postmagmatic Processes. Petropavlovsk-Kamchatsky, 1–41 [in Russian].

Palache, C., Berman, H. and Frondel, C. (1951) *The System of Mineralogy of James Dwight Dana and Edward Salisbury Dana, Yale University 1837–1892*, II, 101–107. John Wiley and Sons, Inc., New York.

Pouchou, J.L. and Pichoir, F. (1991) Quantitative analysis of homogeneous or stratified microvolumes applying the model "PAP". Pp. 31–75 in: *Electron Probe Quantitation* (K.F.J. Heinrich and D.E. Newbury, editors). Plenum Press, New York.

Rychagov, S.N., Sokolov, V.N. and Chernov, M.S. (2010) Hydrothermal clays as a high dynamical colloid-disperse mineralogical-geochemical system. *Doklady Akademii Nauk*, **435**, 806–809.

Rychagov, S.N., Nuzhdaev, A.A. and Stepanov, I.I. (2014) Mercury as an indicator of modern ore-forming gas-hydrothermal systems, Kamchatka. *Geochemistry International*, **52**, 131–143.

Rychagov, S.N., Sergeeva, A.V. and Chernov, M.S. (2017) Mineral specific associations of hydrothermal clays (Southern Kamchatka). *Doklady Akademii Nauk*, **477**, 1–6.

Sajó, I.E. (2012) Characterization of synthetic voltaite analogues. *European Chemical Bulletin*, **1**(1–2), 35–36.

Scacchi, A. (1873) *Contribuzioni mineralogiche per servire alla storia dell' incendio Vesuviano del Mese di Aprile, 1872. Part 2*., Reale Accademia delle Scienze Fisische e Matematiche Naples, 1–69 [in Italian].

Schaller, W.T. (1933) Ammonioborite, a new mineral. *American Mineralogist*, **18**, 480–492.

Sheldrick, G.M. (2015) Crystal structure refinement with SHELXL. *Acta Crystallographica*, **A71**, 3–8.

Szakáll, S., Sajó, I., Fehér, B. and Bigi, S. (2012) Ammoniomagnesiovoltaite, a new voltaite-related mineral species from Pécs-Vasas, Hungary. *The Canadian Mineralogist*, **50**, 65–72.

Volynets, V.F., Zadorozhnyy, I.L. and Florenskiy, K.P. (1967) Isotopic composition of nitrogen in the Earth's crust. *Geokhimiya*, **5**, 587–593.

Yang, H., Martinelli, L., Tasso, F., Sprocati, A.R., Pinzari, F., Liu, Z., Downs, R.T. and Sun, H.J. (2014) A new biogenic, struvite-related phosphate, the ammonium-analog of hazenite, $(NH_4)NaMg_2(PO_4)_2\cdot 14H_2O$. *American Mineralogist*, **99**, 1761–1766.

Zhitova, E.S., Siidra, O.I., Shilovskikh, V.V., Belakovsky, D.I., Nuzhdaev, A.A. and Ismagilova, R.M. (2017) Ammoniovoltaite, IMA 2017-022. CNMNC Newsletter No. 38, August 2017, page 1035; *Mineralogical Magazine*, **81**, 1033–1038.